UDC 621.56:004.89:502.131.1
DOI https://doi.org/10.15589/znp2026.3(506).23

PHYSICS-INFORMED HYBRID ANOMALY DETECTION AND FAULT DIAGNOSIS FOR AN R744 BOOSTER REFRIGERATION SYSTEM WITH HEAT RECOVERY AND OIL MANAGEMENT

ФІЗИКО-ОРІЄНТОВАНЕ ГІБРИДНЕ ВИЯВЛЕННЯ АНОМАЛІЙ ТА ДІАГНОСТУВАННЯ НЕСПРАВНОСТЕЙ У БУСТЕРНІЙ ХОЛОДИЛЬНІЙ СИСТЕМІ НА R744 З РЕКУПЕРАЦІЄЮ ТЕПЛОТИ ТА СИСТЕМОЮ КОТРОЛЮ МАСТИЛА

Olga Yu. Yakovleva[1]
mlle.olga.yakovleva@gmail.com
ORCID: 0000-0003-4785-9069

Oleksii V. Ostapenko[2]
ostapenkosc@gmail.com
ORCID: 0000-0003-0990-7883

О. Ю. Яковлева[1],
канд. техн. наук, доцент

О. В. Остапенко[2],
канд. техн. наук, інженер-програміст,
незалежний дослідник у галузі холодильних систем

[1]*Odesa National University of Technology, Odesa*
[2]*ITMSFT Group, Odesa*
[1]*Одеський національний технологічний університет, м. Одеса*
[2]*ITMSFT Group, м. Одеса*

Abstract. *Purpose*. To develop and evaluate a physics-informed hybrid anomaly detection and fault diagnosis framework for an R744 booster refrigeration system with heat recovery and oil management by combining thermodynamic modelling and machine learning methods. *Methodology*. The proposed approach integrates thermodynamic feature engineering with two unsupervised machine learning techniques: K-means clustering and an autoencoder neural network. K-means clustering is used to identify global operating-mode deviations, while the autoencoder detects local nonlinear anomalies through reconstruction-error analysis. A hybrid decision logic based on union and intersection rules is applied to improve diagnostic reliability. The framework was validated using a synthetic physics-informed dataset representing seven days of operation with a 10-second sampling interval and including normal operation as well as four fault classes: flash-gas instability, heat-recovery disturbance, oil-return disturbance, and sensor drift. *Findings*. The developed hybrid framework demonstrated high anomaly-detection and fault-diagnosis performance. The Stage-1 anomaly detector achieved Precision = 1.000, Recall = 0.903, and F1-score = 0.949. The Stage-2 diagnostic classifier reached an overall accuracy of 0.992. The results confirmed the capability of the proposed approach to distinguish between different fault mechanisms and associate detected anomalies with physically meaningful thermodynamic processes occurring within the refrigeration system. *Originality*. A physics-informed hybrid fault detection and diagnosis framework for transcritical R744 booster refrigeration systems with heat recovery and oil management is proposed. Unlike conventional purely statistical approaches, the developed methodology combines thermodynamic interpretation with machine learning techniques, enabling both accurate anomaly detection and physically explainable diagnostics. *Practical value*. The proposed framework can be integrated into SCADA and building management systems as a supervisory diagnostic layer for commercial refrigeration applications. The approach supports predictive maintenance, improves system reliability, reduces energy consumption, and facilitates the implementation of intelligent monitoring strategies for low-GWP refrigeration systems.
Key words: R744 booster refrigeration system; fault detection and diagnosis; physics-informed machine learning; k-means clustering; autoencoder; heat recovery; oil management; predictive maintenance.

Анотація. *Мета*. Розробити та оцінити фізико-орієнтований гібридний підхід до виявлення аномалій та діагностування несправностей у бустерній холодильній системі на R744 з рекуперацією теплоти та системою керування мастилом на основі поєднання термодинамічного моделювання та методів машинного навчання. *Методика*. Запропонований підхід поєднує термодинамічне формування ознак із двома методами машинного навчання без учителя: кластеризацією k-means та автоенкодером. Кластеризація використовується для виявлення глобальних змін режимів роботи, тоді як автоенкодер дозволяє визначати локальні нелінійні відхилення на основі похибки реконструкції. Для підвищення достовірності діагностування застосовано комбіновану логіку

об'єднання та перетину результатів обох алгоритмів. Перевірку підходу виконано на синтетичному фізико-орієнтованому наборі даних, що описує сім діб роботи системи з інтервалом дискретизації 10 секунд та включає нормальний режим роботи і чотири типи несправностей: нестабільність флеш-газу, порушення роботи контуру рекуперації теплоти, погіршення повернення мастила та дрейф датчика. *Результати*. Розроблена гібридна система продемонструвала високі показники виявлення аномалій та діагностування несправностей. На першому етапі досягнуто значень *Precision* = 1,000, *Recall* = 0,903 та *F1-score* = 0,949. На другому етапі загальна точність класифікації несправностей становила 0,992. Отримані результати підтвердили здатність запропонованого підходу розрізняти різні типи несправностей та пов'язувати виявлені аномалії з фізичними процесами, що відбуваються в холодильній системі. *Наукова новизна*. Запропоновано фізико-орієнтовану гібридну систему виявлення аномалій та діагностування несправностей для транскритичних бустерних холодильних систем на R744 з рекуперацією теплоти та контролем мастила. На відміну від традиційних статистичних методів, підхід поєднує термодинамічну інтерпретацію з алгоритмами машинного навчання, що забезпечує як високу точність діагностування, так і фізичну пояснюваність результатів. *Практична значимість*. Запропонований підхід може бути інтегрований у системи SCADA та BMS як надбудова для диспетчерського моніторингу комерційних холодильних установок. Використання розробленої системи сприяє реалізації предиктивного обслуговування, підвищенню надійності роботи обладнання, зниженню енергоспоживання та впровадженню інтелектуальних стратегій керування холодильними системами на природних холодоагентах.

Ключові слова: бустерна холодильна система R744; виявлення та діагностування несправностей; фізико-орієнтоване машинне навчання; кластеризація k-means; автоенкодер; рекуперація теплоти; система керування мастилом; предиктивне обслуговування.

PROBLEM STATEMENT

Refrigeration systems form the foundation of Cold Chains [1]. Nowadays, industry needs not only safe but also high-quality cold storage and transportation in a regulated environment to the consumer. Disruptions or inefficient Cold Chain performance lead to product loss, which in own turn contributes to greenhouse gas emissions [1]. Unsafe refrigeration with low-quality food cold storage results in food spoilage [1]. In the EU and among the main global players in the refrigeration market, refrigeration equipment is viewed not just as a technical system element but as a prioritized issue for environmental and energy policies in order to create a sustainable Cold Chain [8, 9, 12].

For commercial refrigeration, the transition toward low-GWP refrigerants has increased interest in R744 [2–5] booster systems, which can reduce direct refrigerant-related emissions while maintaining high refrigeration capacity and allowing heat recovery [5, 8, 20]. However, R744 booster systems are operationally complex [11,13]. Receiver pressure, flash-gas bypass operation, gas-cooler pressure control, compressor staging, oil return, and heat-recovery activation interact under changing load and ambient conditions [17, 20]. In such systems, a small deviation in one subsystem can propagate into compressor work, discharge temperature, COP degradation, or unstable receiver operation. This creates a practical need for diagnostic tools that are both data-driven and physically interpretable [6, 7, 15].

Objectives:

1. Defines a feature-based representation of the R744 booster system using thermodynamic states, control variables, and operational indicators relevant to flash-gas, heat-recovery, oil-return, and sensor-drift disturbances.

2. Develops a hybrid Stage-1 anomaly-detection logic that combines k-means clustering for global operating-mode shifts with an autoencoder for local nonlinear deviations.

3. Implements a Stage-2 fault-diagnosis procedure that classifies detected anomalous samples into physically interpretable fault categories.

4. Evaluates the framework using detection metrics, per-class diagnostic performance, and PCA-based visualization of operating regimes.

5. Discusses how the diagnostic outputs can be integrated into supervisory control, energy auditing, and predictive-maintenance workflows for low-GWP refrigeration systems.

This work makes the following contributions:

– A physics-informed hybrid FDD workflow for R744 booster refrigeration systems with heat recovery and oil-management disturbances.

– A proposal of complementary global vs. localized anomaly detection, showing when clustering or autoencoder methods provide advantages within diagnostic.

– An anomaly fault mapping can be thermodynamically understandable, linking anomaly patterns to refrigeration mechanisms (flash-gas behavior, HR pressure effects, oil-return irregularities, sensor drift).

Together, these contributions support the development of interpretable AI-assisted diagnostics for low-GWP refrigeration systems without reducing the problem to a purely statistical black-box classification task [6, 7, 14, 15].

LITERATURE REVIEW

Literature Review. Among the enhancements, AI presents itself as a new and reliable tool for energy efficiency improvement. Scientists [14] note that AI can help to meet the environmental goals of the EU

Green Deal regulation, amendment to the Monreal Protocol [8, 9] more rapidly. In HVAC and refrigeration applications, AI models together with feedforward neural networks, radial basis function networks, neuro-fuzzy systems, and recurrent networks have demonstrated good performance in prediction, control, and fault detection [6, 7, 15]. However, challenges remain concerning cost, interpretability, and robustness under real-world system conditions [6, 15].

Unsupervised Machine Learning was used for refrigeration-system diagnostics. K-means clustering and autoencoder-based models were applied as the principal unsupervised approaches for system anomaly detection. K-means was initially formulated by MacQueen [16] and later widely formalized by Jain [17]. Fan et al. [18] demonstrated its reliability for system-mode transition identification as well as clustering operational modes in chiller and HVAC systems.

Autoencoders represented efficient performance for nonlinear localized deviation detection. Wang et al. [19] deployed the sparse autoencoder model in order to enhance the fault-detection procedure for the system. Researchers found out that feature extraction based on Deep Learning quite improves diagnostic-system performance in comparison with conventional techniques [6, 15, 19]. Rajabi et al. [20] provided clustering comparison and reconstruction approaches. Transversely, HVAC fault datasets showed that the unsupervised model developed performed better than conventional diagnostics based on rules [20]. In their own turn, supervised HVAC fault-detection methods use labeled both normal and faulty data in order to train decision trees, SVMs, SVR, and NN models [6, 7, 15]. But their performance for real fault data is limited by undersupply, instability, and cost. That leads to dependency on simulated or obsolete datasets. Semi-supervised techniques moderate this dependency with the help of incorporated overflowing data together with the training set steadily expanding [6, 7]. Though, it happens at higher computational cost. Clustering and PCA unsupervised methods can provide a practical variant through normal data together with defining hidden operational-pattern usage [17, 18].

RESEARCH GAPS

Current research gaps include limited evaluation of Machine Learning hybrid unsupervised approaches combining clustering (global anomalies) and Autoencoders (local nonlinear anomalies) [6, 7, 15], insufficient mapping of anomaly signatures to physical refrigeration mechanisms (e.g., HR pressure shifts, oil-return faults, flash-gas instability) in R744 systems [11, 13], and a lack of operational-scale validation for R744 refrigeration systems with heat recovery and oil management [10–13]. This study addresses these gaps by developing and validating a hybrid K-means plus Autoencoder anomaly detection framework intended for real-world R744 booster refrigeration systems within performance objectives linked to sustainability [8, 13, 14].

AIM OF THE STUDY

The aim of this study is to develop and evaluate a physics-informed hybrid anomaly-detection and fault-diagnosis framework for an R744 booster refrigeration system with heat recovery and oil-management monitoring. The framework combines K-means clustering, autoencoder reconstruction error, hybrid decision logic, and fault-type classification on a synthetic dataset calibrated to representative supermarket operating behaviour.

METHODS, OBJECT OF THE STUDY, SUBJECT OF THE STUDY

A hybrid anomaly detection framework was developed for the R744 booster refrigeration system. The system is equipped with the following elements: MT and LT compressors, a gas cooler, an intermediate-pressure receiver, a flash-gas bypass, a heat recovery (HR) heat exchanger, and an oil management system [11, 13]. Data preprocessing, thermodynamic modelling, Unsupervised Machine Learning, and hybrid decision logic are included in the proposed methodology [6, 7, 15].

The object of the study is an R744 booster refrigeration system with heat recovery and oil management operating under representative supermarket conditions [11, 13]. **The subject of the study** is operational fault (anomaly) detection and diagnosis. Both global thermodynamic deviations and localized nonlinear disturbances are identified using a Hybrid Unsupervised Machine Learning approach. This approach combines K-means clustering and deep Autoencoder reconstruction error analysis [16–20].

SYSTEM CONFIGURATION AND OPERATING PRINCIPLE

The R744 booster (two-stage) refrigeration system is shown in Fig. 1. The system is designed for medium-temperature (MT) chilled-food and low-temperature (LT) frozen-food applications [11–13]. During system development, recommendations from the scientific literature and international refrigeration safety standards were taken into account [10, 11, 13].

To enable integrated cooling and heating, a heat-recovery heat exchanger is installed between the gas-cooler outlet and the intermediate-pressure receiver inlet [11, 13]. The heat exchanger cools a secondary water loop from 12 °C to 7 °C, supporting the building's air-conditioning demand [11,12]. Such an arrangement allows the utilization of waste heat and improves overall system energy performance under favourable operating conditions [11, 13].

This configuration can provide approximately 50–250 kW of recoverable thermal capacity at ambient temperatures below 20–25 °C [11, 13]. However, at higher

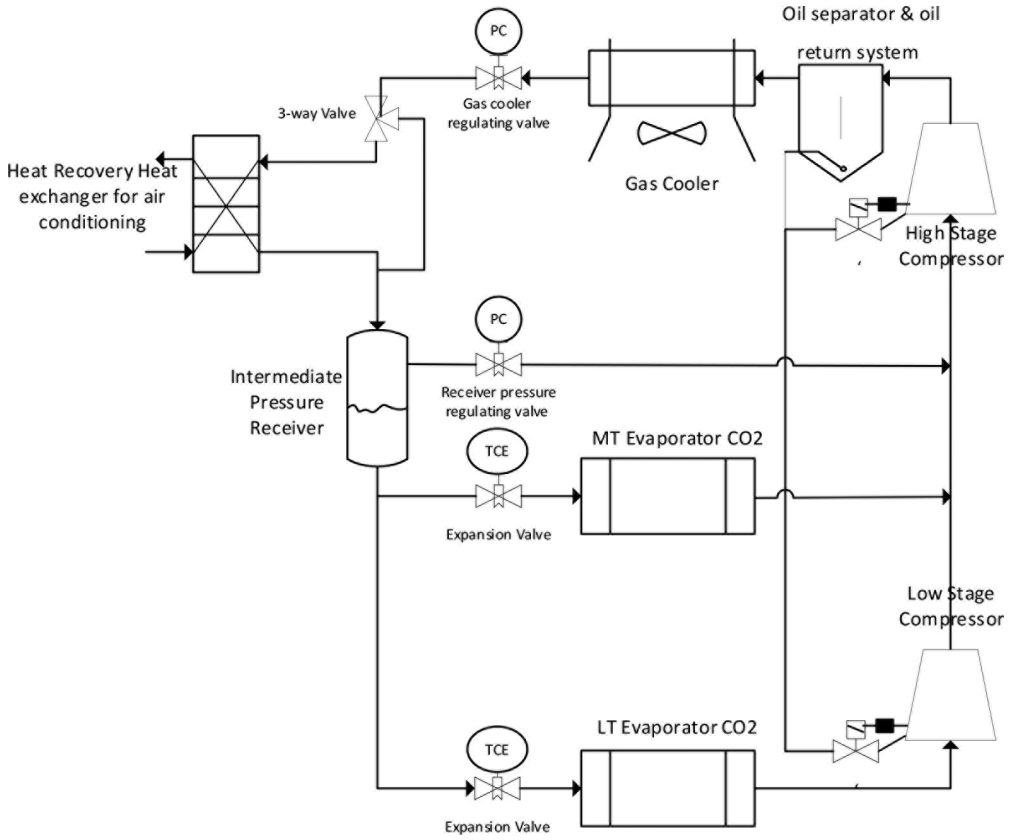


Fig. 1. Booster R744 refrigeration system with heat recovery and oil management (*provided by industry*)

Table 1. Compact operating assumptions and diagnostic role of the retained variables

Block	Retained modelling values	Diagnostic role
Cooling-load scale	LT load 60 kW; MT load 140 kW; total evaporator load 200 kW	Defines the representative supermarket operating scale and the cooling-load baseline
Temperature levels	LT evaporation −25 °C; MT evaporation 0 °C; gas-cooler outlet 35 °C	Sets the baseline thermodynamic state for pressure, superheat, and discharge-temperature features
Pressure levels	Gas-cooler pressure 95 bar; receiver pressure 35–40 bar	Used for high-side, receiver-stability, and flash-gas-instability indicators
Performance indicators	COPsys = 2.2; compressor power 90.9 kW; heat rejection 290.9 kW	Provides COP-related and energy-balance variables for anomaly detection
Heat-recovery assumptions	Heat-recovery fraction 0.5; useful recovered heat 145.5 kW; water ΔT 30–35 K	Supports heat-recovery disturbance features based on pressure, temperature, valve position, and COP deviation
Flow and compression assumptions	MT/LT mass flow 0.78/0.50 kg·s^{-1}; isentropic efficiency 0.75 for MT and LT stages	Links load, compressor work, and discharge-temperature behaviour in the synthetic generator
Inventory and receiver assumptions	CO_2 charge ≈1000 kg; receiver liquid mass ≈200 kg; liquid volume ≈0.22 m^3	Provides the physical context for receiver and oil-return related diagnostic signatures
Diagnostic variables	18-feature vector: pressures, temperatures, superheat, COP, receiver stability, and valve positions	Defines the input space used by k-means, autoencoder detection, and multiclass SVM diagnosis

outdoor temperatures, the performance of transcritical R744 systems may deteriorate because of increased gas-cooler pressure and reduced cycle efficiency [10, 13]. The investigated supermarket application is intended for the climatic conditions of Vinnytsia, Ukraine, characterized by winter temperatures down to approximately –20 °C and summer peak temperatures up to +32 °C, making seasonal heat recovery particularly relevant [10, 11, 13].

OPERATING CONTEXT AND FEATURE SET

Table 1 summarizes the modelling assumptions retained for the diagnostic dataset. In this article, these values are used as calculation inputs for physically

meaningful diagnostic variables rather than as a separate equipment-selection or seasonal-performance table. The feature set links measured or simulated pressure, temperature, valve-position, superheat, heat-recovery, and COP-related variables to the operating mechanisms expected in a supermarket R744 system [11, 13].

SYNTHETIC DATASET AND FAULT SCENARIOS

The diagnostic [21] workflow was evaluated on a synthetic physics-informed dataset generated in MATLAB. The final calculation script represents seven days of operation with a 10 s sampling interval, giving 60,480 samples. Each sample is described by an 18-dimensional feature vector.

The feature vector includes gas-cooler pressure, receiver pressure, MT and LT suction pressures, gas-cooler outlet temperature, MT and LT suction temperatures, MT and LT discharge temperatures, heat-recovery outlet temperature, MT and LT superheat, gas-cooler approach temperature, instantaneous COP, receiver stability index, high-pressure valve position, flash-gas bypass valve position, and heat-recovery valve position. The selected variables reflect key thermodynamic, control, and performance indicators commonly used for monitoring and diagnostics of transcritical R744 refrigeration systems [11, 13].

The dataset contains five operating labels: normal operation and four fault classes. The fault classes were selected because they correspond to physically plausible disturbances in R744 booster systems with heat recovery and oil management [11, 13].

The simulated fault scenarios are:

1) flash-gas instability, represented by receiver-pressure oscillations, MT superheat variation, flash-gas bypass fluctuation, and increased receiver-stability index;

2) heat-recovery disturbance, represented by high-pressure valve and heat-recovery valve deviations, increased gas-cooler pressure, higher discharge temperatures, and reduced instantaneous COP;

3) oil-return disturbance, represented by low-frequency discharge-temperature oscillations, increased MT suction temperature, and increased MT superheat;

4) sensor drift, represented by a gradual bias in MT suction temperature, accompanied by a smaller superheat shift and an apparent COP deviation.

Only healthy samples were used to define the normal feature distribution for unsupervised detection. This reflects the practical situation in which labelled fault data are limited, while normal operating data are more readily available from SCADA or BMS histories.

Because the dataset is synthetic, the results should be interpreted as simulation-based validation of the diagnostic workflow. Field validation on measured operating data remains a required step before deployment [6, 7, 15].

K-MEANS CLUSTERING ANOMALY SCORE

The K-means clustering algorithm was selected as the first-stage unsupervised anomaly detection method because of its ability to identify global shifts in system operating conditions through distance-based partitioning of the feature space [16–18].

The normal data training set is partitioned into K clusters by minimizing:

$$\min_{\{c_k\},\{z_i\}} J = \sum_{i=1}^{N_{train}} \left\| \tilde{x}_i - c_{z_i} \right\|_2^2, \quad (1)$$

where $z_i \in \{1, \ldots, K\}$ is the cluster label of sample *i*.

For any sample *j* (train or test), the K-means anomaly score is the Euclidean distance to its nearest centroid:

$$S_{k-means}(j) = \min_{k \in \{1,\ldots,K\}} \left\| \tilde{x}_j - c_k \right\|_2. \quad (2)$$

A threshold $\tau_{k\text{-}means}$ is derived from the empirical distribution of $s_{k\text{-}means}$ on healthy data:

$$a_{k-means}(j) = \begin{cases} 1, \rightarrow s_{k-means}(j) > \tau_{k-means}(K-means_anomaly) \\ 0, \rightarrow otherwise \end{cases}. \quad (3)$$

AUTOENCODER FOR NONLINEAR LOCAL ANOMALY DETECTION

The autoencoder was trained on healthy operating data in order to capture nonlinear relationships in the feature space [6, 15, 19]. The autoencoder maps the input $\tilde{x}_i$ to a low-dimensional latent vector h_i and back:

$$h_i = f(W_e \tilde{x}_i + b_e), \quad (4)$$

$$\hat{x}_i = g(W_d h_i + b_d), \quad (5)$$

where *f*(.) and *g*(.) are element-wise nonlinear activation functions such as hyperbolic tangent function tanh; trainable parameters are the W_e, W_d, encoder and decoder weight matrices; b_e, b_d bias vectors.

Training minimizes the mean squared reconstruction error on healthy data [19, 20]:

$$\min_{\theta} \frac{1}{N_{train}} \sum_{i=1}^{N_{train}} \left\| \tilde{x}_i - \hat{x}_i \right\|_2^2, \quad (6)$$

where $\theta = \{W_e, W_d, b_e, b_d\}$.

The Autoencoder provides the anomaly score after training the reconstruction error for any *j* sample:

$$s_{autoencoder}(j) = \left\| \tilde{x}_j - \hat{x}_j \right\|_2^2. \quad (7)$$

With a threshold $\tau_{autoencoder}$ derived from the reconstruction error empirical distribution:

$$a_{autoencoder}(j) = \begin{cases} 1, \rightarrow s_{autoencoder}(j) > \tau_{autoencoder}(Autoencoder_anomaly) \\ 0, \rightarrow otherwise \end{cases}. \quad (8)$$

Hybrid anomaly indicator Stage 1 Detection. The union (high-sensitivity) and intersection (high-precision)

hybrid indicators combine clustering-based and reconstruction-based anomaly information to improve robustness of unsupervised fault detection [6, 7, 15, 20].

$$a_{\cup}(j) = Ind(a_{k\text{-}means}(j) = 1 \vee a_{autoencoder}(j) = 1); \quad (9)$$

$$a_{\cap}(j) = Ind(a_{k\text{-}meamns}(j) = 1 \wedge a_{autoencoder}(j) = 1). \quad (10)$$

where *Ind*(.) is the indicator function: 1 if the condition is true and 0 otherwise.

HYBRID STAGE-1 DETECTION LOGIC

Before anomaly detection, all features are standardized using the mean and standard deviation of the healthy training subset. This prevents variables with large numerical ranges from dominating distance-based and reconstruction-based scores [18–20].

The first detector is *k-means* clustering trained on healthy operation. It captures global operating-mode deviations by measuring the distance between each sample and the nearest normal-operation centroid. Samples with excessive centroid distance are flagged as global anomalies [16–18].

The second detector is an autoencoder trained on healthy operation. It learns the nonlinear manifold of normal R744 booster behaviour and uses reconstruction error as an anomaly score. This detector is expected to be more sensitive to local nonlinear deviations that may not be far from a k-means centroid [19, 20].

The two detector outputs are combined using union and intersection logic. The union output is suitable for early warning because it accepts anomalies detected by either method. The intersection output is more conservative and is used as the high-confidence Stage-1 detection signal because it requires agreement between the two methods [6, 7, 15, 20].

This hybrid structure preserves the complementary behaviour of the detectors: k-means is sensitive to global operating shifts, while the autoencoder is sensitive to reconstruction inconsistency in nonlinear feature relationships [18–20].

STAGE-2 FAULT DIAGNOSIS AND PERFORMANCE METRICS

Samples identified by the high-confidence Stage-1 intersection logic are passed to the second diagnostic stage [6, 15, 20]. In this article, the diagnostic stage is treated as a multiclass classification problem in which anomalous samples are assigned to one of four fault classes: flash-gas instability, heat-recovery disturbance, oil-return disturbance, or sensor drift [6, 7, 15].

The classifier is trained and tested only on anomalous non-normal samples. A hold-out split is used for the diagnostic stage so that classification accuracy and per-class metrics are evaluated on samples not used during classifier training [6, 15].

Detection performance is evaluated using true positives, false positives, false negatives, true negatives, precision, recall, and F1-score. For Stage-2 diagnosis, the same precision, recall, and F1 definitions are computed separately for each fault class.

The purpose of this two-stage structure is to separate the detection question (whether a sample is anomalous) from the diagnostic question (which physical fault mechanism is most likely responsible).

This separation is important for supervisory control because early-warning alarms and maintenance recommendations require different confidence levels [14, 15].

Performance metrics are computed for binary detection (normal vs. anomalous):

$$Precision = (TP)/(TP + \mathrm{FP}), \quad (11)$$

$$Recall = (TP)/(TP + FN), \quad (12)$$

$$F1 = (2 \cdot Precision \cdot Recall)/(Precision + Recall). \quad (13)$$

The same equations are applied per class, treating one class as positive and the rest as negative; F1 scores can be macro-averaged across all fault types for multiclass diagnosis [6, 7, 15].

INTEGRATION WITH THERMODYNAMIC MODELLING AND SUPERVISORY WORKFLOW

The developed thermodynamic model provides the physical baseline for the anomaly-detection framework. Expected pressures, temperatures, compressor work, heat-recovery indicators, and COP-related quantities are used to construct physically interpretable features [11, 13]. The machine-learning detectors then compare observed or simulated operating behaviour with this feature-space representation of normal operation [6, 7, 15].

The hybrid anomaly-detection pipeline is formalized by the software architecture shown in Fig. 2. Raw field measurements can be represented by the Sensor, Measurement, and DataAcquisition classes; the thermodynamic model reconstructs the system state; and the FeatureExtractor module generates the numerical vector consumed by the K-means and autoencoder detectors [6, 15, 21].

The *FeatureExtractor* module can transform each *Measurement* or *State* pair into a high dimensional *FeatureVector*. This vector constitutes the numerical representation consumed by downstream detectors. Both K-means and Autoencoder implementations inherit from the polymorphic *IDetector* interface. This interface standardizes anomaly scoring (score(x)) and anomaly classification (isAnomaly(score)) [20, 21].

The *AnomalyDecision* module can evaluate detected anomalies. This module applies hybrid decision logic and invokes the *AlertService* for system operator notification. A *Repository* can store all intermediate artifacts measurements, computed states, features, and anomaly labels in order to ensure traceability, reproducibility, and support for future retraining [14, 21].

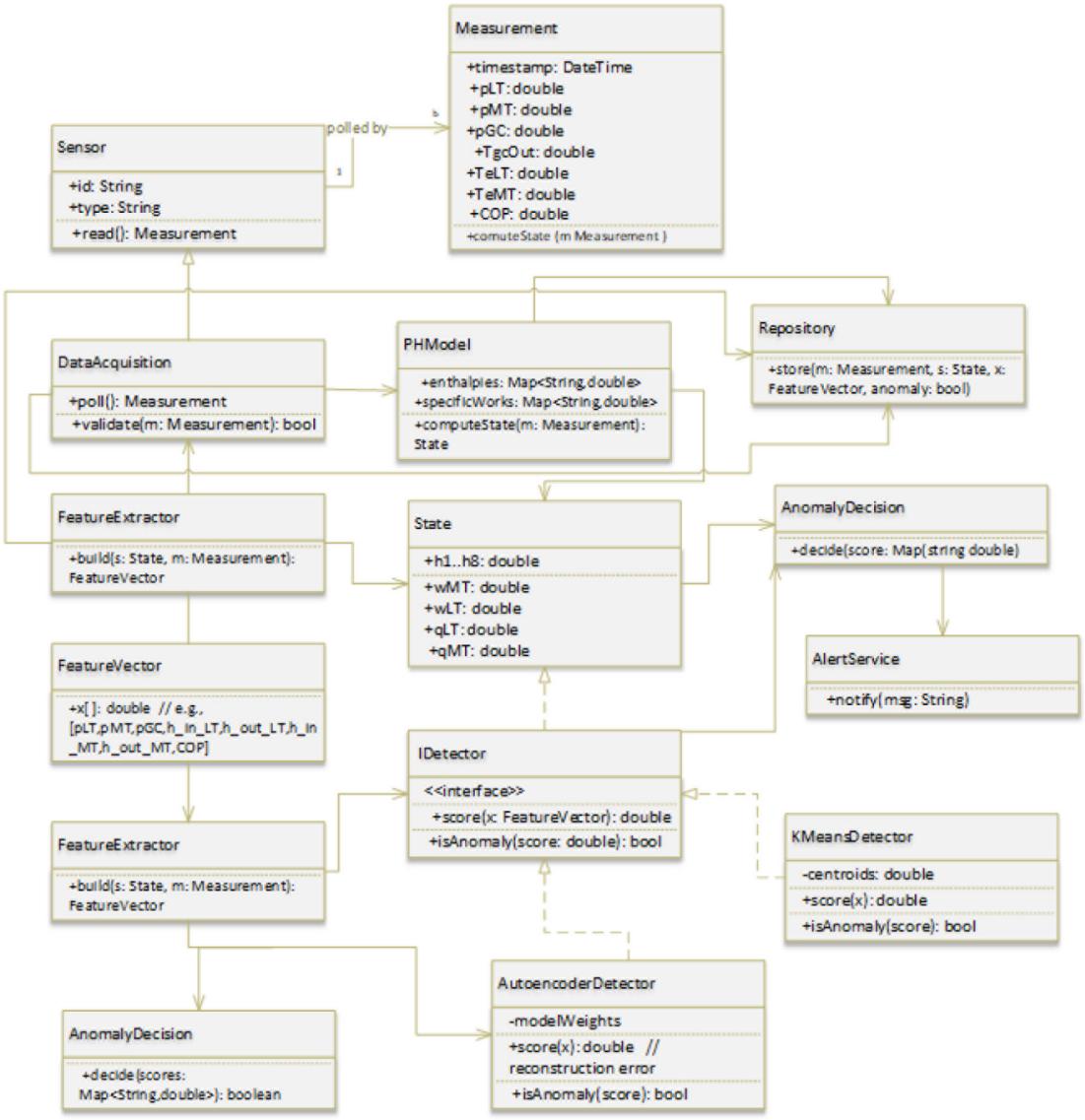


Fig. 2. Physics-informed hybrid anomaly-detection workflow for the R744 booster refrigeration system

The workflow links Sensors → Data Acquisition → P–h/thermodynamic model → Feature Extraction → K-means and Autoencoder detectors → Anomaly Decision → Alert Service and Repository.

RESULTS AND DISCUSSION

Dataset Structure and Diagnostic Separability. This section reports the fault-detection and diagnostic results obtained for the physics-informed synthetic dataset. The discussion is focused on feature separability, Stage-1 anomaly detection, Stage-2 fault diagnosis, and the operational interpretation of the detector outputs.

The synthetic physics-informed dataset represents seven days of R744 booster operation at a 10 s sampling interval, giving 60,480 samples. Each sample is described by the 18-feature vector defined in the methodology section. The dataset includes normal operation and four fault classes: flash-gas instability, heat-recovery disturbance, oil-return disturbance, and sensor drift.

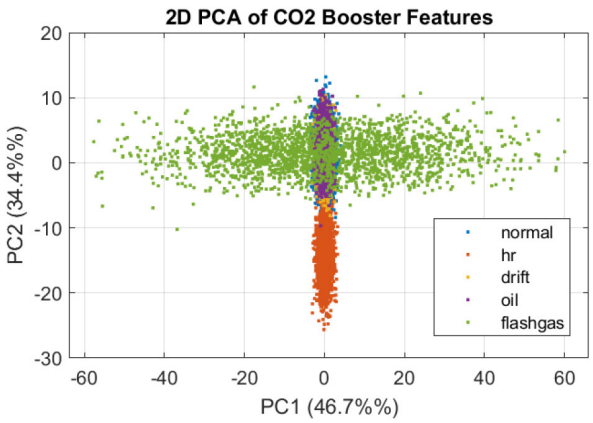


Fig. 3. 2D PCA plot

Principal Component Analysis was used as an auxiliary visualization tool to assess whether the engineered thermodynamic features separate normal and faulty regimes. The first three principal components retained more than 95 % of the total variance in the current dataset. The resulting projection confirmed that the simulated fault regimes are not arbitrary statistical noise: they form physically interpretable deviations associated with receiver-pressure behaviour, heat-recovery valve action, oil-return degradation, and gradual sensor bias.

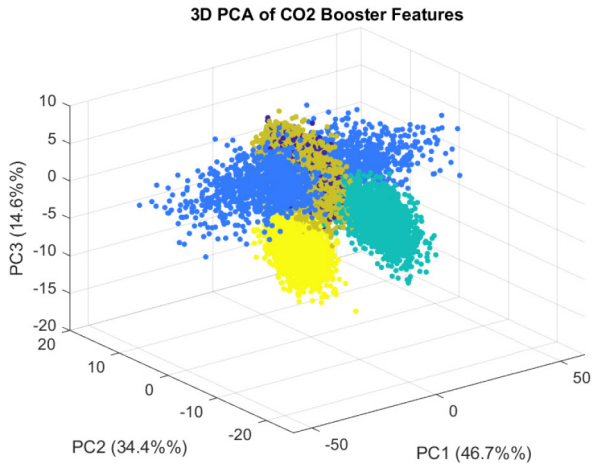


Fig. 4. 3D PCA plot

Stage-1 Hybrid Anomaly Detection. The Stage-1 anomaly detector combines thermodynamic feature engineering with two unsupervised indicators: K-means clustering for global operating-mode displacement and a sparsity-regularized autoencoder for nonlinear local reconstruction errors. The synthetic dataset reproduces characteristic R744 booster patterns, including MT and LT evaporation behaviour, gas-cooler pressure modulation, flash-gas bypass fluctuations, oil-return effects, and receiver-pressure regulation.

The PCA projections in Fig. 3 and Fig. 4 are therefore used only as diagnostic visualization, not as a separate classifier. They confirm that the selected feature set contains physically meaningful separation between normal operation and the four simulated fault families.

Stage-1 detection used the conservative intersection of the K-means and autoencoder outputs. This choice intentionally reduces false alarms because a sample is accepted as a high-confidence anomaly only when both detectors agree. In the current synthetic run, the intersection detector produced TP = 43,690, FP = 5, FN = 4,695, and TN = 12,090. These values correspond to $Precision$ = 1.000, $Recall$ = 0.903, and $F1$ = 0.949 after rounding.

The result indicates that the detector is highly selective: false alarms are almost eliminated, while most fault samples are still captured. The remaining false negatives are consistent with the selected conservative logic and are expected mainly near fault onset, recovery intervals, or weakly expressed disturbances where only one detector responds strongly.

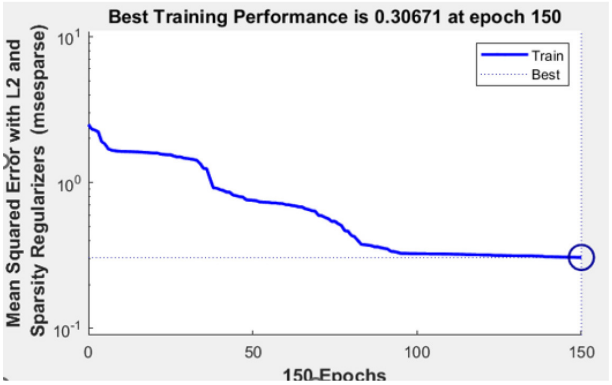


Fig. 5. Autoencoder training performance for reconstruction-error learning on healthy operating data

Stage-2 Fault Diagnosis Performance. Stage-2 diagnosis was evaluated only for non-normal anomalous samples. This separation prevents the diagnostic classifier from being dominated by normal operating data and makes the reported performance directly relevant to fault identification. In the current run, the diagnostic stage achieved an overall accuracy of 0.992.

The class-level F1 scores were 0.997 for flash-gas instability, 1.000 for heat-recovery disturbance, 0.983 for oil-return disturbance, and 0.982 for sensor drift. Heat-recovery disturbance was the most clearly separated class because it produces simultaneous changes in gas-cooler pressure, valve position, discharge temperature, and instantaneous COP. Oil-return disturbance and sensor drift were more difficult because both can appear as gradual temperature and superheat deviations, especially when the fault magnitude is moderate.

Interpretation of Detector Complementarity. The two unsupervised detectors showed complementary behaviour. K-means was more sensitive to global operating-mode displacement, including receiver-pressure excursions and high-side changes associated with heat-recovery operation. The autoencoder was more sensitive to nonlinear reconstruction inconsistency and therefore better reflected localized disturbances such as sensor drift or oil-return degradation.

For supervisory diagnostics, this complementarity is more useful than either detector alone. The union output can be retained as an early-warning signal when sensitivity is more important than alarm selectivity. The intersection output is more appropriate for high-confidence alarms, maintenance prioritization, and Stage-2 fault classification.

Practical Considerations for Supervisory-Control Integration. The proposed diagnostic workflow can be integrated into SCADA or BMS environments as a supervisory layer rather than as a direct low-level controller. Measurements are converted into physically

interpretable features, anomaly scores are computed by independent detectors, and the final decision layer determines whether an alarm should be issued or whether the sample should be routed to fault diagnosis.

Practical deployment requires periodic retraining after changes in refrigerant charge, oil-management settings, heat-recovery control strategy, or sensor calibration. A sampling interval of 1–5 s is sufficient for online monitoring in most supervisory applications, while the 10 s interval used in the synthetic validation is adequate for demonstrating the proposed diagnostic logic.

Table 2. Stage-2 fault-diagnosis performance for the final 18-feature R744 booster FDD dataset

Fault class	Precision	Recall	F1-score
Flash-gas instability	–	–	0.997
Heat-recovery disturbance	–	–	1.000
Oil-return disturbance	–	–	0.983
Sensor drift	–	–	0.982
Overall Stage-2 accuracy			0.992

Overall, the results support the feasibility of a physics-informed hybrid FDD framework for R744 booster refrigeration systems. The workflow does not replace thermodynamic interpretation; instead, it uses thermodynamic feature engineering to make machine-learning alarms more traceable and operationally meaningful.

CONCLUSION

This work developed and evaluated a physics-informed hybrid FDD framework for an R744 booster refrigeration system with heat recovery and oil-management monitoring. The framework combines thermodynamic feature engineering, K-means clustering, autoencoder reconstruction error, hybrid decision logic, and a second-stage fault-diagnosis procedure. The final synthetic dataset represents seven days of operation with a 10 s sampling interval and an 18-feature vector describing pressures, temperatures, valve positions, superheat, COP-related indicators, and receiver stability.

The Stage-1 intersection strategy provided a conservative high-confidence anomaly signal. For the current run it produced *Precision* = 1.000, *Recall* = 0.903, and $F1 = 0.949$, indicating that false alarms were almost eliminated while most fault samples were still detected. The remaining missed samples are consistent with weakly expressed or transitional fault states where only one unsupervised detector responds strongly.

The Stage-2 diagnostic stage assigned anomalous samples to four physically interpretable fault classes: flash-gas instability, heat-recovery disturbance, oil-return disturbance, and sensor drift. The overall Stage-2 accuracy was 0.992. The strongest separation was obtained for heat-recovery disturbance, while oil-return disturbance and sensor drift remained more challenging because both can appear as gradual temperature and superheat deviations.

The results support the use of hybrid unsupervised diagnostics as a supervisory layer for low-GWP commercial refrigeration systems. The proposed workflow does not replace thermodynamic interpretation; instead, it makes machine-learning alarms more traceable by linking anomaly scores to pressure regulation, heat-recovery operation, oil-return behaviour, and sensor bias. Practical deployment will require field validation, periodic retraining after control or charge changes, and calibration of alarm thresholds for the target SCADA or BMS environment.

REFERENCES

[1] Friedman-Heiman, A., & Miller, S. A. (2024). The impact of refrigeration on food losses and associated greenhouse gas emissions throughout the supply chain. *Environmental Research Letters, 19*(6), 064038. https://doi.org/10.1088/1748-9326/ad4c7b

[2] International Organization for Standardization. (2024). *ISO 817:2024. Refrigerants – Designation and safety classification*. ISO.

[3] European Committee for Standardization. (2020). *EN 378-1, EN 378-2, EN 378-3, EN 378-4: Refrigerating systems and heat pumps – Safety and environmental requirements*. CEN.

[4] ASHRAE. (2022). *ANSI/ASHRAE Standard 15: Safety standard for refrigeration systems* and *ANSI/ASHRAE Standard 34: Designation and safety classification of refrigerants*. ASHRAE.

[5] International Institute of All-Natural Refrigeration. (2019). *Natural refrigerants for a sustainable future*. IIAR Green Paper.

[6] Bi, J., et al. (2024). AI in HVAC fault detection and diagnosis: A systematic review. *Energy Reviews, 3*(2), 100071. https://doi.org/10.1016/j.enrev.2024.100071

[7] Zhou, S. L., et al. (2023). A comprehensive review of the applications of machine learning for HVAC. *DeCarbon, 2*, 100023. https://doi.org/10.1016/j.decarb.2023.100023

[8] European Parliament and Council of the European Union. (2024). *Regulation (EU) 2024/573 of the European Parliament and of the Council of 7 February 2024 on fluorinated greenhouse gases*. EUR-Lex. https://eur-lex.europa.eu/eli/reg/2024/573/oj/eng

[9] United Nations. (2016). *Amendment to the Montreal Protocol on Substances that Deplete the Ozone Layer (Kigali Amendment)*. United Nations Treaty Collection. https://treaties.un.org/Pages/ViewDetails.aspx?src=IND&mtdsg_no=XXVII-2-f&chapter=27&clang=_en

[10] International Institute of Refrigeration. (2025, January 27). *GL2024: Improving the performance of R744 refrigeration systems at high ambient temperatures*. https://iifir.org/en/news/gl2024-improving-the-performance-of-r744-refrigeration-systems-at-high-ambient-temperatures

[11] Karampour, M., & Sawalha, S. (2017). Energy efficiency evaluation of integrated CO_2 trans-critical systems in supermarkets: A field measurement and modelling analysis. *International Journal of Refrigeration, 82*, 470–486. https://doi.org/10.1016/j.ijrefrig.2017.06.002

[12] Sengupta, A., Gullo, P., Khorshidi, V., & Dasgupta, M. S. (2025). Transcritical R744 supermarket refrigeration system integrated with a heat-driven ejector chiller. *Applied Sciences, 15*(6), 2955. https://doi.org/10.3390/app15062955

[13] Gullo, P., Hafner, A., & Banasiak, K. (2018). Transcritical R744 refrigeration systems for supermarket applications: Current status and future perspectives. *International Journal of Refrigeration, 93*, 269–310. https://doi.org/10.1016/j.ijrefrig.2018.07.001

[14] Gailhofer, P., et al. (2021). *The role of artificial intelligence in the European Green Deal*. European Parliament. https://www.europarl.europa.eu/RegData/etudes/STUD/2021/662906/IPOL_STU(2021)662906_EN.pdf

[15] Adelekan, D. S., Ohunakin, O. S., & Paul, B. S. (2022). Artificial intelligence models for refrigeration, air conditioning and heat pump systems. *Energy Reports, 8*, 8451–8466. https://doi.org/10.1016/j.egyr.2022.06.062

[16] MacQueen, J. (1967). Some methods for classification and analysis of multivariate observations. In *Proceedings of the Fifth Berkeley Symposium on Mathematical Statistics and Probability* (Vol. 1, pp. 281–297). University of California Press.

[17] Jain, A. K. (2010). Data clustering: 50 years beyond k-means. *Pattern Recognition Letters, 31*(8), 651–666. https://doi.org/10.1016/j.patrec.2009.09.011

[18] Fan, C., Xiao, F., Zhao, Y., & Wang, J. (2018). Discovering gradual patterns in building operations for improving building energy efficiency. *Applied Energy, 224*, 116–123. https://doi.org/10.1016/j.apenergy.2018.04.118

[19] Wang, Z., Zhong, J., Li, J., & Xia, C. (2019). Fault diagnosis of air-conditioning refrigeration systems based on sparse autoencoder. *International Journal of Low-Carbon Technologies, 14*(4), 487–492. https://doi.org/10.1093/ijlct/ctz034

[20] Rajabi, F., & McArthur, J. J. (2023). Unsupervised learning for fault detection of HVAC systems: An OPTICS-based approach for terminal air handling units. *arXiv*. http://arxiv.org/abs/2312.11405

[21] International Organization for Standardization. (2003). *ISO 13374-1:2003. Condition monitoring and diagnostics of machines – Data processing, communication and presentation – Part 1: General guidelines*. ISO. https://www.iso.org/standard/21832.html

СПИСОК ВИКОРИСТАНОЇ ЛІТЕРАТУРИ

[1] Friedman-Heiman, A., & Miller, S. A. (2024). The impact of refrigeration on food losses and associated greenhouse gas emissions throughout the supply chain. *Environmental Research Letters, 19*(6), 064038. https://doi.org/10.1088/1748-9326/ad4c7b

[2] International Organization for Standardization. (2024). *ISO 817:2024. Refrigerants – Designation and safety classification*. ISO.

[3] European Committee for Standardization. (2020). *EN 378-1, EN 378-2, EN 378-3, EN 378-4: Refrigerating systems and heat pumps – Safety and environmental requirements*. CEN.

[4] ASHRAE. (2022). *ANSI/ASHRAE Standard 15: Safety standard for refrigeration systems* and *ANSI/ASHRAE Standard 34: Designation and safety classification of refrigerants*. ASHRAE.

[5] International Institute of All-Natural Refrigeration. (2019). *Natural refrigerants for a sustainable future*. IIAR Green Paper.

[6] Bi, J., et al. (2024). AI in HVAC fault detection and diagnosis: A systematic review. *Energy Reviews, 3*(2), 100071. https://doi.org/10.1016/j.enrev.2024.100071

[7] Zhou, S. L., et al. (2023). A comprehensive review of the applications of machine learning for HVAC. *DeCarbon, 2*, 100023. https://doi.org/10.1016/j.decarb.2023.100023

[8] European Parliament and Council of the European Union. (2024). *Regulation (EU) 2024/573 of the European Parliament and of the Council of 7 February 2024 on fluorinated greenhouse gases*. EUR-Lex. https://eur-lex.europa.eu/eli/reg/2024/573/oj/eng

[9] United Nations. (2016). *Amendment to the Montreal Protocol on Substances that Deplete the Ozone Layer (Kigali Amendment)*. United Nations Treaty Collection. https://treaties.un.org/Pages/ViewDetails.aspx?src=IND&mtdsg_no=XXVII-2-f&chapter=27&clang=_en

[10] International Institute of Refrigeration. (2025, January 27). *GL2024: Improving the performance of R744 refrigeration systems at high ambient temperatures*. https://iifir.org/en/news/gl2024-improving-the-performance-of-r744-refrigeration-systems-at-high-ambient-temperatures

[11] Karampour, M., & Sawalha, S. (2017). Energy efficiency evaluation of integrated CO_2 trans-critical systems in supermarkets: A field measurement and modelling analysis. *International Journal of Refrigeration, 82*, 470–486. https://doi.org/10.1016/j.ijrefrig.2017.06.002

[12] Sengupta, A., Gullo, P., Khorshidi, V., & Dasgupta, M. S. (2025). Transcritical R744 supermarket refrigeration system integrated with a heat-driven ejector chiller. *Applied Sciences, 15*(6), 2955. https://doi.org/10.3390/app15062955

[13] Gullo, P., Hafner, A., & Banasiak, K. (2018). Transcritical R744 refrigeration systems for supermarket applications: Current status and future perspectives. *International Journal of Refrigeration, 93*, 269–310. https://doi.org/10.1016/j.ijrefrig.2018.07.001

[14] Gailhofer, P., et al. (2021). *The role of artificial intelligence in the European Green Deal*. European Parliament. https://www.europarl.europa.eu/RegData/etudes/STUD/2021/662906/IPOL_STU(2021)662906_EN.pdf

[15] Adelekan, D. S., Ohunakin, O. S., & Paul, B. S. (2022). Artificial intelligence models for refrigeration, air conditioning and heat pump systems. *Energy Reports, 8*, 8451–8466. https://doi.org/10.1016/j.egyr.2022.06.062

[16] MacQueen, J. (1967). Some methods for classification and analysis of multivariate observations. In *Proceedings of the Fifth Berkeley Symposium on Mathematical Statistics and Probability* (Vol. 1, pp. 281–297). University of California Press.

[17] Jain, A. K. (2010). Data clustering: 50 years beyond k-means. *Pattern Recognition Letters, 31*(8), 651–666. https://doi.org/10.1016/j.patrec.2009.09.011

[18] Fan, C., Xiao, F., Zhao, Y., & Wang, J. (2018). Discovering gradual patterns in building operations for improving building energy efficiency. *Applied Energy, 224*, 116–123. https://doi.org/10.1016/j.apenergy.2018.04.118

[19] Wang, Z., Zhong, J., Li, J., & Xia, C. (2019). Fault diagnosis of air-conditioning refrigeration systems based on sparse autoencoder. *International Journal of Low-Carbon Technologies, 14*(4), 487–492. https://doi.org/10.1093/ijlct/ctz034

[20] Rajabi, F., & McArthur, J. J. (2023). Unsupervised learning for fault detection of HVAC systems: An OPTICS-based approach for terminal air handling units. *arXiv*. http://arxiv.org/abs/2312.11405

[21] International Organization for Standardization. (2003). *ISO 13374-1:2003. Condition monitoring and diagnostics of machines – Data processing, communication and presentation – Part 1: General guidelines*. ISO. https://www.iso.org/standard/21832.html

© Яковлева О. Ю., Остапенко О. В.
Дата першого надходження статті до видання: 19.06.2026
Дата прийняття статті до друку після рецензування: 21.07.2026
Дата публікації (оприлюднення) статті: 02.11.2026



Стаття поширюється на умовах ліцензії відкритого доступу (CC BY 4.0)